Journal of Physics:
Conference Series

PURPOSE-LED PUBLISHING™

PAPER • **OPEN ACCESS**

A Deep Learning Model for Automated Segmentation of Fluorescence Cell images

To cite this article: Musa Aydın *et al* 2022 *J. Phys.: Conf. Ser.* **2191** 012003

View the article online for updates and enhancements.

You may also like

- Characterization of a hybrid nanowire-MEMS force sensor using direct actuation
Bartosz Pruchnik, Krzysztof Kwoka, Tomasz Piasecki et al.
- Skin-on-a-chip technologies towards clinical translation and commercialization
Nilufar Ismayilzada, Ceren Tarar, Sajjad Rahmani Dabbagh et al.
- 3D bioprinted glioma models
Defne Yigci, Misagh Rezapour Sarabi, Merve Ustun et al.

Enabling Electrochemistry Inside and Outside the Lab

PalmSens

Discover our diverse range of Potentiostats engineered to support your research wherever it takes you

- Intuitive software for Windows and Android
- Proven in over 4000 scientific publications
- Single-channel and multi-channel
- Benchtop, portable and wearable

Discover More



This content was downloaded from IP address 88.255.99.33 on 27/10/2026 at 07:39

A Deep Learning Model for Automated Segmentation of Fluorescence Cell images

Musa Aydın[1*], Berna Kiraz[1,2], Furkan Eren[2], Yiğit Uysallı[2,3], Berna Morova[3], Selahattin Can Ozcan[4], Ceyda Acilan[4,5], and Alper Kiraz[2,3,4,6]

[1]Department of Computer Engineering, Fatih Sultan Mehmet Vakif University, Istanbul, Turkey
[2]Optofil Inc., Istanbul, Turkey
[3]Department of Physics, Koç University, Istanbul, Turkey
[4]Koç University Research Center for Translational Medicine (KUTTAM), Istanbul, 34450, Turkey
[5]School of Medicine, Koç University, Istanbul, 34450, Turkey
[6]Department of Electrical and Electronics Engineering, Koç University, Istanbul, Turkey

E-mail: maydin@fsm.edu.tr[1*], bkiraz@fsm.edu.tr[1], akiraz@ku.edu.tr[3]

Abstract. Deep learning techniques bring together key advantages in biomedical image segmentation. They speed up the process, increase the reproducibility, and reduce the workload in segmentation and classification. Deep learning techniques can be used for analysing cell concentration, cell viability, as well as the size and form of each cell. In this study, we develop a deep learning model for automated segmentation of fluorescence cell images, and apply it to fluorescence images recorded with a home-built epi-fluorescence microscope. A deep neural network model based on U-Net architecture was built using a publicly available dataset of cell nuclei images [1]. A model accuracy of 97.3% was reached at the end of model training. Fluorescence cell images acquired with our home-built microscope were then segmented using the developed model. 141 of 151 cells in 5 images were successfully segmented, revealing a segmentation success rate of 93.4%. This deep learning model can be extended to the analysis of different cell types and cell viability.

1. Introduction

Manual image segmentation performed by an expert is considered as the gold standard; however, it is a time-consuming process, which constantly requires expert intervention and can result in high variations due to different interpretations of experts. Besides, it is prone to human errors due to the background noise that may reduce contrast of the objects to be segmented. These shortcomings of manual segmentation can be overcome by deep learning techniques which have been widely used for biomedical image segmentation to speed up the process, increase the reproducibility, and reduce the workload in manual segmentation.

Convolutional neural network (CNN) is a deep neural network that extracts important features of an input with the application of different kernels. CNNs have been applied to many biomedical image segmentation problems such as cell segmentation, brain vessel segmentation, and brain tumor segmentation [2, 3, 4, 5, 6]. Among different CNN architectures, U-Net model


Content from this work may be used under the terms of the Creative Commons Attribution 3.0 licence. Any further distribution of this work must maintain attribution to the author(s) and the title of the work, journal citation and DOI.
Published under licence by IOP Publishing Ltd

is often selected as the architecture of choice for biomedical image segmentation due to its high performance and accuracy [7, 8].

In this study, we develop a deep learning model based on U-Net architecture for automated segmentation of fluorescence cell images. We trained our model using a publicly available dataset that contains images of cell nuclei as well as corresponding ground truths [1], and obtained a training accuracy of 97.3%. We then applied the trained model to automated segmentation of cell images obtained with a home-built epi-fluorescence microscope. Fluorescence images were acquired using U2OS cells stained with DAPI (6-diamidino-2-phenylindole) that enables imaging of nuclear DNA. 141 of 151 cells were successfully segmented in 5 fluorescence images, corresponding to a segmentation success rate of 93.4%.

2. Experimental Study

In this section we describe the dataset used for segmentation of cell images with the deep neural network together with the deep learning method and algorithm. For the images in the dataset, image pre-processing was applied before training in the deep neural network. The pre-processing steps were histogram matching and median filtering. Histogram matching is the process of transforming the histogram of one image to match with the histogram of another image [9]. In our implementation, the histogram of each image in the dataset was matched to the histogram function distribution of the image with the highest average light intensity value. This way, contrast differences between images were reduced. After that, a 3×3 median filter was applied to all images in order to eliminate the background noise. The dataset used in this study and all the developed codes can be accessed at github[1].

2.1. Dataset

In this study we used the publicly available dataset of cell nuclei images [1] which consisted of 670 images encoded with Portable Network Graphics format (*.png*) defined in RGB color space with corresponding binary ground truths that are manually created by experts. Figure 1 shows sample images and ground truths from the dataset.

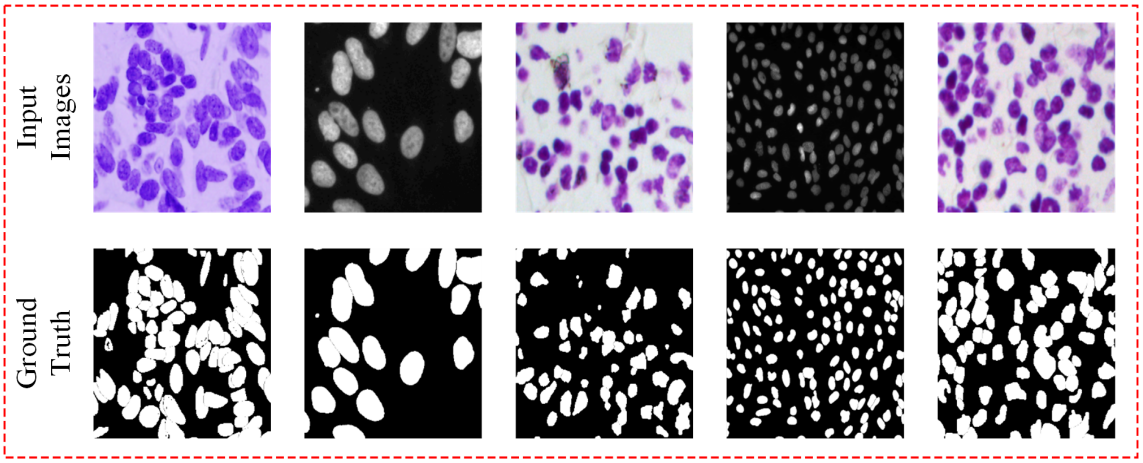


Figure 1. Exemplary input images and the corresponding ground truths from the dataset used for cell segmentation.

The sizes of the images in the cell dataset are different from each other. Thus, all images were resized to 256×256 in the image pre-processing step. 80% of the 670 images in the cell dataset

[1] https://github.com/msaaydin/U-net-Segmentation

was randomly selected for model training while the remaining 20% of was used for tests. Each image selected for training or tests also has ground truths available in the dataset. For ground truths, merging was done in the image pre-processing step. An image found in the original data set was manually segmented as follows. Initially, multiple ground truth images were created and saved corresponding to each cell in a reference image. As a result, more than one segmented ground truth images were created for a reference image. The ground truths corresponding to all images were then merged into a single image during the image pre-processing step, and the data set was updated. This way a new updates dataset was obtained. The new updated dataset can be accessed on github[1].

2.2. Method

In this study we employed the U-Net convolutional neural network that has a proven track record in numerous biomedical image segmentation studies in the literature [10]. The U-Net model employed, consisted of two main parts: Encoder and decoder. The main purpose of the encoder and decoder architecture used in the U-Net model is to enable concatenation of the information at different abstraction levels. Encoder reduces the dimensions of the features maps produced by convolutional layers using max pooling operations. This way low resolution, higher level information maps are constructed. These maps contain detailed features of the objects in the image which are sufficient for defining them while lacking many details. These details are then recovered by concatenating the information layers generated by the encoder with high resolution, lower level information maps generating with upsampling operations of the decoder.

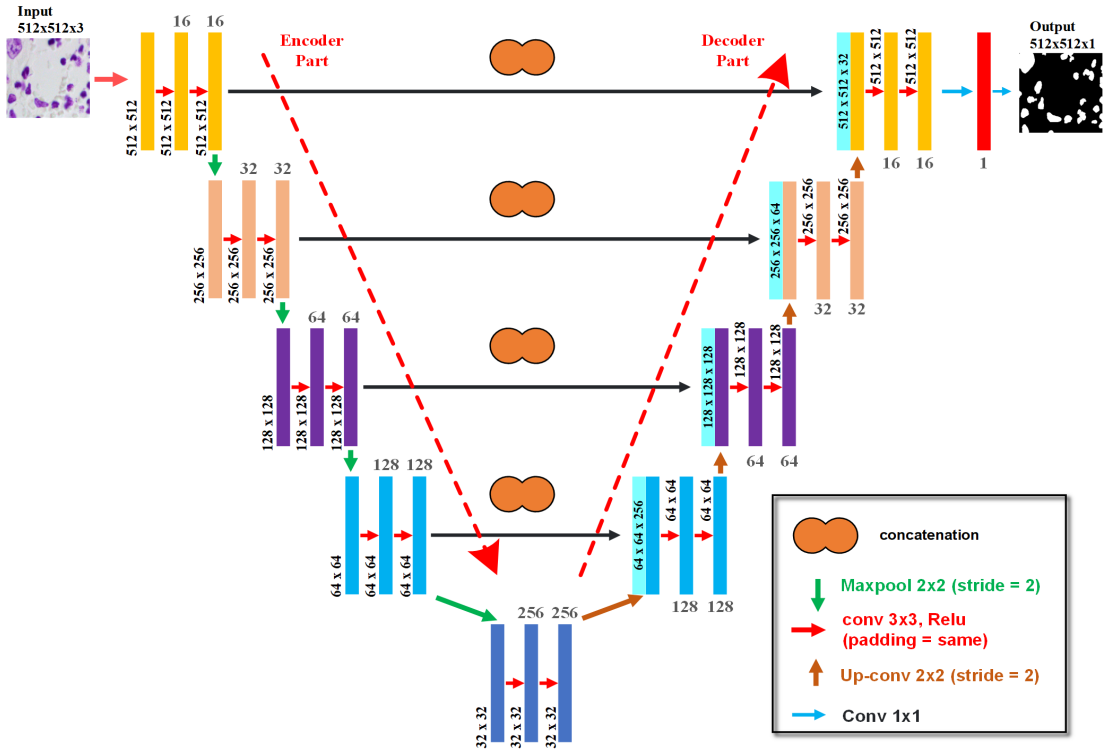


Figure 2. Diagram showing the encoder and decoder parts of the U-Net model developed for cell segmentation.

The first part, i.e. encoder, is known as the contracting path. Contracting path is a convolutional network containing steps where convolutions are performed, reducing the input

dimensions. At each step of the contracting path, the data size is downsampled with max pooling operations (stride=2). Each step in the contracting path contains 2 convolutional layers with 3×3 filter size, employing rectified linear unit (ReLU) activation with zero padding. Feature size at the input layer is 16 and this number is doubled at each step of the contracting path. The second part of the U-Net model, i.e. decoder, is the expansive path where, at each step, the results obtained from 2×2 upsampling (stride=2) are concatenated with feature channels of the contracting path that are obtained from the same steps. Following concatenation, each step of the expansive path employs 2 convolutional layers with 3×3 filter size, employing ReLU activation with zero padding. After each upsampling step in the expansive path, the number of feature channels is halved. Hence, the contracting and expansive paths are symmetrical. In the final step of the U-Net model, a 1×1 convolution is implemented in order to extract the segmentation map from 16 feature maps. Due to the limited data size, each convolutional layer is followed by dropout operation with 0.2 ratio in order to prevent overfitting. All the operations (e.g. convolution, max pooling, upsampling, donwsapmling) used in the U-Net model constructed in this work are shown in Fig. 2.

Computational experiments were performed using the Google colab infrastructure and keras-tensorflow (version 2.4.1, python version = 3.7) library. In our U-Net network architecture, 16 feature maps were extracted in the first step, and propagated with 4 downsampling steps where the size of the feature map is doubled at each step (Fig. 2). U-Net model hyperparameters were selected as: Optimizer: Adam, epoch: 40, loss: binary crossentropy, metrics: [accuracy], learning rate: 0.001. 10% of the dataset was used for model validation together with a batch size of 4 at each iteration.

3. Results and Discussion

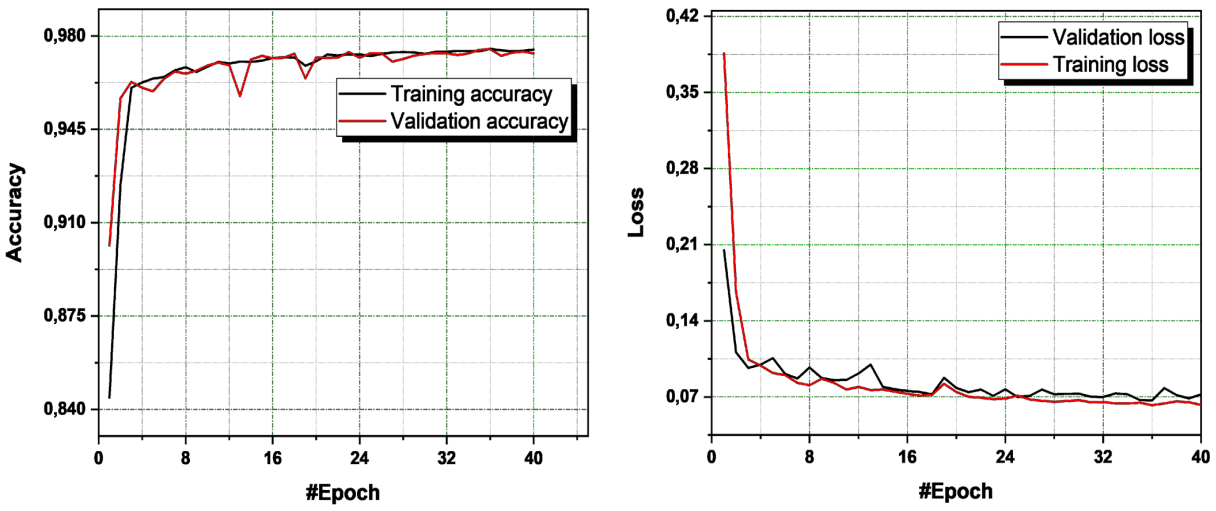


Figure 3. Changes of (a) accuracy and (b) loss with number of batches in cell segmentation during U-Net model training.

Figure 3 shows the accuracy and loss curves as a function of number of batches obtained during training and validation cycles. A very high accuracy of 97.3% was obtained with tests at the end of model training. The accuracy value was obtained as the average of accuracies obtained from 10 tests conducted.

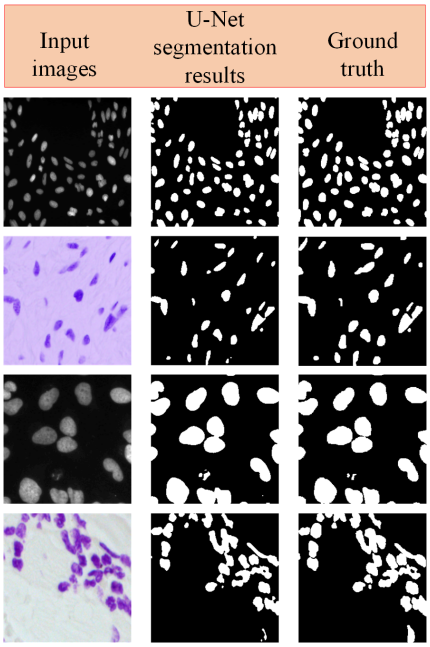


Figure 4. Exemplary input images and ground truths used for U-Net model training together with U-Net segmentation results.

Exemplary input images and U-Net segmentation results obtained with our model together with corresponding ground truths are shown in Fig. 4. A very good match is visible between the U-Net segmentation results and ground truths, as expected from the high accuracy values obtained in model training. We then applied our trained model to five fluorescence microscopy cell images recorded in our laboratory. These fluorescence images are recorded using a custom epi-fluorescence microscope which employs LED excitation at 4 colors (wavelengths of LEDs are 405, 488, 532, 633 nm), a 20X microscope objective (Nikon 20X, NA=0.4), and a CMOS camera detector (Basler daA3840-45um). Fluorescence images were collected from U2OS cells which

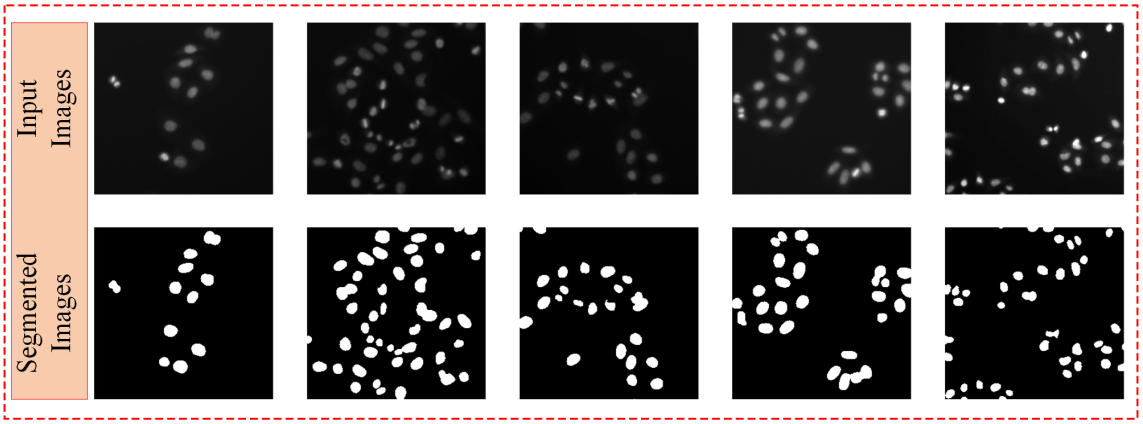


Figure 5. Input images obtained using our home-built epi-fluorescence microscope and the corresponding segmented images obtained as a result of segmentation with the U-Net model developed in this study.

were grown on coverslips and fixed with ice cold methanol at -20°C for 10 min, washed 3 times

with PBS, and mounted on glass slides using Vectashield mounting medium containing DAPI (4,6-diamidino-2-phenylindole) (Vector Laboratories; H-1000-10). Segmentation results of these images are shown in Fig. 5. A very high accuracy in cell segmentation was also achieved with this dataset of 5 images. Out of a total of 151 cells in the images shown in Fig. 5, 141 of them were correctly segmented, corresponding to a segmentation success rate of 93.4%.

In conclusion, in this study we developed a U-Net model for cell segmentation and trained our model using a publicly available dataset of cell images. An accuracy of 97.3% was obtained at the end of model training. We then employed this trained model to cell segmentation using 5 fluorescence images recorded in our experimental setup, and successfully segmented 141 of 151 cells, corresponding to a segmentation success rate of 93.4%. This work can be extended to segmentation of images that contain different cell types and to classification for cell viability analysis. We are also planning to use such a U-Net based image segmentation approach to other biomedical image processing problems including brain vasculature analysis.

Acknowledgments

We acknowledge financial supports from TÜBİTAK (Project No: 7190434) and KOSGEB. A. Kiraz acknowledges partial support from the Turkish Academy of Sciences (TÜBA).

References

[1] "Cell nuclei data set," https://www.kaggle.com/c/data-science-bowl-2018/data, last access: 01-03-2021.
[2] R. Hollandi, A. Szkalisity, T. Toth, E. Tasnadi, C. Molnar, B. Mathe, I. Grexa, J. Molnar, A. Balind, M. Gorbe *et al.*, "nucleaizer: a parameter-free deep learning framework for nucleus segmentation using image style transfer," *Cell Systems*, vol. 10, no. 5, pp. 453–458, 2020.
[3] M. Habibzadeh, M. Jannesari, Z. Rezaei, H. Baharvand, and M. Totonchi, "Automatic white blood cell classification using pre-trained deep learning models: Resnet and inception," in *Tenth international conference on machine vision (ICMV 2017)*, vol. 10696. International Society for Optics and Photonics, 2018, p. 1069612.
[4] M. Delgado-Ortet, A. Molina, S. Alférez, J. Rodellar, and A. Merino, "A deep learning approach for segmentation of red blood cell images and malaria detection," *Entropy*, vol. 22, no. 6, p. 657, 2020.
[5] M. R. K. Mookiah, S. Hogg, T. J. MacGillivray, V. Prathiba, R. Pradeepa, V. Mohan, R. M. Anjana, A. S. Doney, C. N. Palmer, and E. Trucco, "A review of machine learning methods for retinal blood vessel segmentation and artery/vein classification," *Medical Image Analysis*, p. 101905, 2020.
[6] M. Havaei, A. Davy, D. Warde-Farley, A. Biard, A. Courville, Y. Bengio, C. Pal, P.-M. Jodoin, and H. Larochelle, "Brain tumor segmentation with deep neural networks," *Medical image analysis*, vol. 35, pp. 18–31, 2017.
[7] O. Ronneberger, P. Fischer, and T. Brox, "U-net: Convolutional networks for biomedical image segmentation," in *International Conference on Medical image computing and computer-assisted intervention*. Springer, 2015, pp. 234–241.
[8] M. Livne, J. Rieger, O. U. Aydin, A. A. Taha, E. M. Akay, T. Kossen, J. Sobesky, J. D. Kelleher, K. Hildebrand, D. Frey *et al.*, "A u-net deep learning framework for high performance vessel segmentation in patients with cerebrovascular disease," *Frontiers in neuroscience*, vol. 13, p. 97, 2019.
[9] S. P. Ehsani, H. S. Mousavi, and B. H. Khalaj, "Iterative histogram matching algorithm for chromosome image enhancement based on statistical moments," in *2012 9th IEEE International Symposium on Biomedical Imaging (ISBI)*. IEEE, 2012, pp. 214–217.
[10] Z. Liu, "Retinal vessel segmentation based on fully convolutional networks," *arXiv preprint arXiv:1911.09915*, 2019.